# Soft merging in early-type galaxies (*)

M. CAPACCIOLI [1][2], G. LONGO [1], P. BÖHM [3]
G. RICHTER [3] and M. D'ONOFRIO [4]

[1] *Osservatorio Astronomico di Capodimonte - Via Moiariello 16, I-80131 Napoli, Italy*
[2] *Dipartimento di Scienze Fisiche, Università Federico II - Napoli, Italy*
[3] *Astrophysikalisches Institut Potsdam*
*An der Sternwarte 16, Potsdam-Babelsberg D-14482, Germany*
[4] *Dipartimento di Astronomia, Università di Padova*
*Vicolo Osservatorio 5, I-35122 Padova, Italy*

(ricevuto il 30 Luglio 1996)

**Summary.** — Statistical, photometric, and kinematical arguments suggest that encounters, accretion, and merging of galaxies are likely the key mechanisms for the formation of present-day ellipticals. While major merger events leave strong and clearly measurable signatures, those left by minor (or "soft") ones are usually rather tricky to observe. In this paper we present a new image-filtering technique capable to detect weak photometric signatures (down to 5% of the local value of the surface brightness) of structures which may be interpreted as signatures of past accretion phenomena. By applying this technique to a sample of 28 early-type galaxies observed with the ESO-NTT telescope, we have revealed faint structures such as nuclear disks, ripples, bars, distorted disks, warps, etc., in more than 90% of the galaxies. The revealed structures are also capable to explain some anomalies in the photometric properties which were known to exist by means of more traditional techniques.

PACS 98.20 – Stellar clusters and associations.
PACS 07.05.Pj – Image processing.
PACS 98.52 – Normal galaxies; extragalactic objects and systems (by type).
PACS 98.62.Mw – Infall, accretion, and accretion disks.
PACS 01.30.Cc – Conference proceedings.

## 1. – Introduction

Due to their lack of clearly/easily detectable morphological structures, early-type galaxies, *i.e.* ellipticals and lenticulars, were numbered for a long time amongst the

(*) Paper presented at the Fourth Italian-Korean Meeting on Relativistic Astrophysics, Rome-Gran Sasso-Pescara, July 9-15, 1995.

simplest objects in the extragalactic zoo: ellipticals were thought to be spheroidal systems flattened by rotation, while lenticulars were a sort of simplified spirals lacking in gas, spiral arms, and star-forming regions.

This peaceful scenario came abruptly to an end in the seventies when both theory and observations begun to show that real objects are far more complex systems. On the theoretical side Toomre [1] showed, by means of *N*-body simulations, that E galaxies could form as coalescence products of two or more objects trapped with low relative velocity into the same potential well. On the observational side, Bertola and Capaccioli [2] discovered that the apparent flattening of spheroidal galaxies was not supported by rotation only, thus opening the way to the idea of anisotropic velocity distributions and triaxiality [3]. Triaxial potentials—which offer a rather natural explanation of the observed isophotal twisting—while on the one hand added a further degree of freedom to the problem of determining the intrinsic structure of dynamically "hot" systems, on the other hand prompted a substantial amount of studies on the stability of stellar orbits. Soon it became clear that in such systems stable closed orbits are allowed in two planes only: the plane containing the long and intermediate axis and that containing the short and intermediate one (cf. [4]).

The detection of axisymmetric, extended structures (or sub-components) in early-type galaxies became then a topic of the uttermost relevance: stable structures being tools to constraint the dynamical models [5-7] and unstable structures shedding light on the time scale of secondary-evolution events [8-11].

The main questions to be answered seem therefore to be the following:

i) What is the relative frequency of major (*i.e.* between equal-mass objects) and minor merger events?

ii) Which type of sub-components do exist in early-type galaxies and how frequent are they?

iii) What is their dynamical status and origin of such sub-components or, in other words, are these structures genetic or rather evolutionary varieties?

Direct evidence that a fair fraction of ellipticals might originate from major mergers comes from the observations of some clear-cut cases of ongoing mergers (*e.g.*, NGC 7552 [12]), as well as from the statistics of minor axis rotations. These suggests that some ellipticals are intrinsically triaxial in shape and tend to rotate slowly, a behaviour currently understood in terms of mergers between equal-disk galaxies through *N*-body simulations [13].

Besides simple statistical arguments which favour minor accretion events with respect to major ones, the most relevant observational evidences in support of minor accretion events come from the photometric and kinematical detection of a wealth of weak structures or sub-components in the inner and intermediate galaxy regions ([1]), which are not easily understood otherwise.

The first detected structures in E-type galaxies were symmetric dust lanes [14]. In a recent work van Dokkum and Franx [15], using archival HST material, have shown that the dust is present in almost the totality of early-type galaxies and that, even on the smallest scale (*i.e.* with relaxation time shorter than $10^8$ y) the dust is not

([1]) We assume as inner and intermediate regions those comprised within $0.1\,r_e$ and $2.0\,r_e$. The very inner regions ($r \leqslant 0.1\,r_e$) have usually a sub-arcsecond size and cannot be effectively studied with seeing limited ground-based observations.

completely relaxed. The dust turns out to be usually associated with cold and ionized gas which is often observed to be kinematically decoupled (*i.e.* with misaligned spins or even counter-rotating) from the stellar component of the parent galaxy (see the review by Kormendy and Djorgovski [16]).

Another type of features, sharp-edged and arc-shaped, are known to exist in ellipticals [17-19], lenticulars and even galaxies of later morphological types [20]. Even though some confusion seems to exist between the terms "shells" and "ripples", we prefer to follow Schweizer and Seitzer's [21] notation in using "ripples" for all sharp-edged structures since: i) the term is descriptive and does not prejudice the geometric interpretation of the features; ii) both morphologies share the same formation mechanism as debris from a small disk galaxy accreted by a large elliptical, but "shells" are just a particular case produced by radial accretion events [9] which obviously have a much smaller cross-section than the non-radial accretions which are responsible for the formation of "ripples".

"Ripples" are usually detected as periodic trends in the residuals of the observed surface brightness profiles with respect to some best-fitting photometric law, such as, for instance, the $r^{1/4}$ law [22], or in model-subtracted maps of the light distribution. Both these methods tend to favour the detection of "ripples" of intermediate inclination with respect to the observer.

Stellar disks are a third type of structure recently found in $E$ galaxies. Their existence was first suspected by Capaccioli ([23]; but see also [24]) who found that some deviations from a pure $r^{1/4}$ law detected in the intermediate regions of the luminosity profiles of some ellipticals may be best explained by assuming that these objects harbour a stellar disk. The claim of Capaccioli was that such disks should be rather abundant since, owing to either intrinsic faintness or unfavorable orientation, most of them likely escape morphological detection.

By simple modelling Rix and White [25] confirmed that disks contributing as much as 20% of the total galaxy luminosity could easily be missed by any trivial morphological and photometric recognition.

Additional observational evidence was provided by Nieto *et al.* [26] who found that, out of nearly 100 galaxies, 12% had photometric properties which could be understood only in terms of at least two distinct photometric components. In many cases the nature of the second component (whether a stellar disk, a bar or a ring) proved however not easy to disentangle.

A different method to detect disk-like features in E galaxies was introduced by Bender *et al.* [27]. Making use of the fourth Fourier component, $a_4$, of the residuals of the isophotal fit to ellipses, Bender found the existence, isophote-wise, of at least two types of elliptical galaxies: those with an excess of light in the direction of the photometric major axis (called "disky" ellipticals), and those presenting a deficit of light in the same direction (named "boxy"). This phenomenological dichotomy was found to correlate with other galaxian properties such as X-ray and radio luminosities, degree of anisotropy, luminosity, etc. [28], thus proving the existence of two distinct physical classes of objects.

It needs to be kept in mind, however, that, even though the most straightforward explanation for the disky isophotes is the presence of a weak disk inside the bulge—and this is surely the case for the large majority of the disky galaxies—analytical one-component mass models in axisymmetric triaxial potentials can also reproduce the same phenomenon without the need for an inner disk [29].

An extensive study of all the signatures left by the occurrence of past merging

events can be found in the works of Schweizer and collaborators, who wanted to quantify the probability of a galaxy of being the product of recent merging through the $\Sigma$ index. Even nuclear features can be identified with HST data as shown in Jaffe *et al.* [30] and related papers.

All the above-mentioned structures make a rather complex scenario the interpretation of which is strongly affected by the lack of homogeneity in the available data, thus implying that statistical parameters such as the rate of occurrence cannot be easily inferred. Additional evidences for the existence of subcomponents produced by accretion events come from the kinematics of the inner galaxy regions (see [4] for a review).

In this paper we present a new method to reveal on photometric grounds the weak structures hidden in early-type galaxies. We discuss the application of this method to a sample of 28 galaxies observed with the ESO-NTT telescope during several observing runs.

After showing that the occurrence of mergers could explain the existence of two families of early-type galaxies, we discuss the Adaptive Laplacian Method used to detect the structures, and we present the data for the individual galaxies. The complex detected morphologies as well as the comparison with the data already available in the literature are reviewed.

## 2. – Families of elliptical galaxies

The existence of two families of early-type galaxies suggested by Bender *et al.* [28] using the above-mentioned $a_4$ parameter is more firmly established in terms of the effective structural parameters ($R_e$, $\mu_e$), where $R_e$ is the linear radius of the galaxy which encloses half the total luminosity and $\mu_e$ is the corresponding surface brightness. In fact, through this approach projection effects acting on the $a_4$ parameter are minimized. Once more it is found that elliptical galaxies segregate into two well-defined groups [31] according to their absolute magnitude. "Bright" ellipticals, *i.e.* objects having $M_B < -19.3$ (adopting $H_0 = 70$ km s$^{-1}$ Mpc$^{-1}$), form a one-parameter family obeying the so-called Hamabe and Kormendy [32] relation, while "ordinary" ellipticals (*i.e.* $M_B > -19.3$) compose a two-parameter family with $M_B > -19.3$ and $R_e < 3$ kpc (see fig. 1).

*A posteriori* one finds that most "ordinary" objects are of the "disky" type and that most "bright" galaxies have "boxy" isophotes. The "bright" galaxies are generally radio loud, X-bright, host active nuclei, etc., while the "ordinary" ones have the opposite properties. In other words, the "bright" *E*'s clearly present a higher degree of activity than less luminous ones [33].

The question of whether this enhancement is due to genetic or rather to evolutionary effects can be addressed by means of simple computations. Spheroids with homologous light distributions have effective parameters $I_e$ (effective intensity) and $R_e$ (effective linear radius) which are linked to the total luminosity by the relation:

$$L_T = s I_e R_e^2 , \tag{1}$$

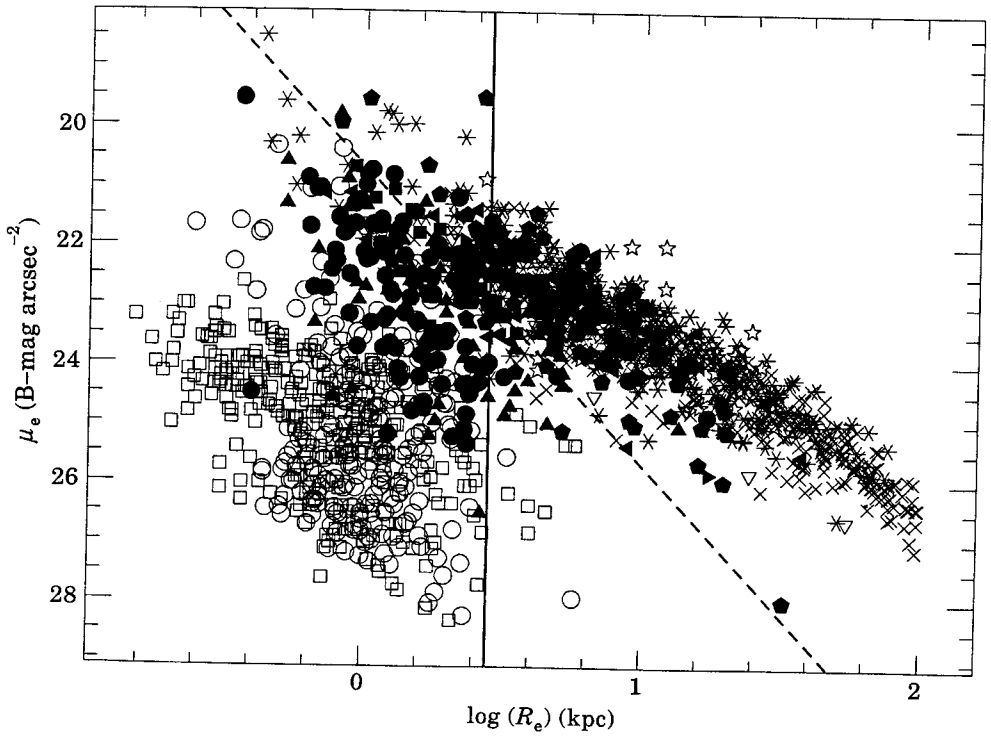


Fig. 1. – The whole distribution of early-type galaxies, bulges of S0 galaxies, dwarf ellipticals and S0's, early-type galaxies in compact groups, brightest cluster galaxies, and galaxies hosting quasars in the ($\log R_e$, $\mu_e$)-plane. Legenda of the different sources: filled circles [34, 35]; filled triangles [36, 37]; filled squares [38]; filled pentagons [39]; crosses [40, 41]; asterisks [42]; open triangles [43, 44]; open stars [45]; open circles [46]; open squares [47]. The oblique dashed line is that of constant luminosity, $M_B = -19.3$, *i.e.* the upper limit of the "ordinary" group. The vertical solid line is the cut-off at $R_e \sim 3$ kpc. Number of points = 1703.

where $s$ is the so-called structural parameter, whose value depends on the shape of the light profile. If we assume that light profiles can be approximated with a Sersic law [48]:

$$I(r) = I_0 \, dex(-r^{1/n}), \tag{2}$$

the numerical calculations show that, in the range $0.6 < n < 10$, the structural parameter is very accurately approximated as [49]

$$\log s = 0.46 \log n + 1.08 . \tag{3}$$

A least-square fit to the "ordinary" members of the Virgo and Fornax cluster gives [49]

$$M_B = -5.66(\pm 0.07) \log R_e + 1.02(\pm 0.01) \mu_e - 40.2(\pm 0.3), \tag{4}$$

where absolute quantities are tuned on a distance modulus of the Virgo cluster equal to 31.3 Mpc. From eq. (1) and the Virial Theorem written as $(L/R)(M/L) \propto \sigma^2$ it is easy to derive

$$L \propto I_e^{-0.81 \pm 0.11} \sigma^{3.58 \pm 0.13} \left( \frac{M}{L} \right)^{-1.79 \pm 0.05} \tag{5}$$

which, in the case of a marginal dependence of $M/L$ on $L$, compares quite well with the Djorgovski and Davis Fundamental Plane [50]:

$$L \propto \langle I \rangle_e^{-0.86} \sigma^{3.45} , \tag{6}$$

where $\langle I \rangle_e$ is the mean surface brightness within the effective isophote. If the "bright" family is added to the "ordinary" one, eqs. (1) and (2) become, respectively,

$$M_B = -5.40(\pm 0.04) \log R_e + 1.00(\pm 0.01) \mu_e - 39.3(\pm 0.3) , \tag{7}$$

and

$$L \propto I_e^{-0.86 \pm 0.06} \sigma^{3.72 \pm 0.08} \left( \frac{M}{L} \right)^{-1.86 \pm 0.03} . \tag{8}$$

The coefficients of $\log R_e$ differ from the expectation for a homologous family with $s = \text{const}$. By writing the structural parameter as $s = u \times R_e^{\gamma}$, where $u$ is a universal constant, $\gamma$ turns out to be 0.16, which implies that $s$ increases with $R_e$ or, in other words, that the light profile must become progressively shallower as $R_e$ stretches. Such a trend was predicted by the results of $N$-body simulations of mergers between equal-mass galaxies [51] and detected by Caon *et al.* [35] who found

$$\log n = 0.51(\pm 0.04) \log R_e + 0.30(\pm 0.03) , \tag{9}$$

for a sample of galaxies in Virgo and Fornax.

## 3. – The adaptive filter

The detection of weak photometric structures in the inner regions of early-type galaxies is badly hampered by the steep and varying slope in the intensity of the underlying galaxy. In the easiest cases these structures show up as small deviations of the isophotes, such as isophotal twisting, by the above-mentioned $a_4$ parameter and by the behaviour of the higher-order Fourier coefficients. Such signatures, however, are not always easy to disentangle one from the other. Exploratory tools usually recommended in the literature are the high-pass stationary (*i.e.* with constant size) filters of the Gradient or Laplacian types, providing the first- and second-order derivatives of the surface brightness distribution. These filters are tuned to detect only one particular scale-length. In the case of filters such as the "Roberts Gradient" or the "Sobel operator" for instance, the scale is the shortest one in the image, as defined by the pixel raster. Another way to construct Laplacian filters is the so-called "Unsharp Masking" technique, which calculates the difference between two versions of the same input image smoothed with two different scale-lengths. In this case the operator is requested to choose the sensitive scale-length beforehand. Again, the scale-length remains constant over the whole image.

An attempt toward extending the scale-length range are the so-called pyramidal or hierarchical filters introduced, for instance, by Burt and Adelson [52]. This technique provides the user with a series of images filtered at successively increasing or decreasing scale-lengths. Once more the user has to extract—by his subjective judgement—the relevant scale-length of the features.

A more effective and user-independent approach is offered by the adaptive filters, *i.e.* filters capable of recognizing the local scale-length of the signal and adapting the filter size to it. The best criterion for detecting a signal depends, in the general case, on the signal itself.

In the present application we make use of the two-dimensional Gradient and Laplace terms (*i.e.* of the first and second derivative of the intensity map of the object), averaged over a spectrum of scale-lengths. The noise spectrum for both terms is estimated in the sky background regions of each frame, while the shortest scale-length at which the local Gradient and Laplace terms exceed the noise significantly, determines the local value of the filter size. The application of this filter for smoothing the noise without degrading the signal has been described elsewhere [53-55]. In what follows we outline for the first time its application as a structure-detecting algorithm.

For the detection of symmetric (roundish) or bar-like structures in the inner and higher signal-to-noise ratio (S/N) regions of the galaxies, the Laplacian filter is more effective, while in the outer low-surface-brightness galaxian regions the Gradient filter is sometimes more effective. Since in the present work we are mainly interested in the inner structures, we provide here only some details on the use of the Laplacian maps.

The interpretation of the Laplacian maps is far from trivial and some specific points need to be stressed.

i) The Laplacian image (hereafter L-image) represents the second derivative, *i.e.* the radius of curvature, of the surface brightness distribution (for convenience, in fig. 2-11, the curvature is inverted: negative values corresponding to concavity and positive values to convexity).

ii) An L-image does not retain any photometric information and must be used only to disentangle structures and to study their morphology. For instance, L-images provide an independent way to estimate the size and trace the geometry of the hidden features, thus helping in masking out the structures in order to model a “clean” galaxy to be subtracted to the original image (cf. the case of NGC 3384, [56]).

iii) Every convex spike—such as a star—is surrounded by a concavity due to the fact that the filter has a square-shaped response. This squared shape, far from being a nuisance, helps in disentangling artifacts from the real structures.

iv) Along the minor axis, and outside the seeing blurred galaxy core, there is almost always a negative signature produced by the concavity of the luminosity profile (cf. the $r^{1/4}$ law which is usually a good approximation of the surface brightness profile). However, since the two-dimensional curvature is the average of the one-dimensional curvatures measured in the two main curvature directions, in elongated systems the very central convex part is more extended along the major axis (in the case of high axis ratios there is no negative curvature along the major axis at all). This effect, has nothing to do with what we call inner disks, which are clearly differentiated from the aforementioned fake-features by their profiles and their

well-defined edges along the main axes. Since it preserves the spatial resolution, the Laplacian morphology (hereafter L-Mor) allows us to detect edge-on or close to edge-on ripples as patches of enhanced emission which are more or less symmetric with respect to the nuclei of the galaxies. It should always be kept in mind, however, that the same Laplacian morphologies may be produced by completely different structures such as, for instance, weak polar rings or bars [56].

## 4. – The data

The CCD images used in this paper were collected during three observing runs with the ESO-NTT through EMMI in the upper red-arm mode. It is worth noticing that the present sample of galaxies is by no means intended to satisfy any special selection criterium in that the targets were originally chosen for another purpose: the study of the surface brightness fluctuations [57].

Details on the runs and on the observations of the individual objects are given elsewhere [58]. Here we limit ourselves to just a few pieces of information. In order to avoid saturation in the central regions of the galaxies, several exposures were taken for each object. The number of exposures as well as the total exposure times differ from object to object. Flat field images were obtained by exposing the CCD at the twilight light. Each frame was pre-processed (removal of the bias and dark, flat-fielding) with the PAFF: Potsdam Advanced Filtering Facility [53, 55]. When more than one frame of comparable quality were available, the individual frames were re-centered and stacked in order to increase the S/N. The resulting frames were then processed through the *Adaptive Algorithm*.

## 5. – The objects

In this paragraph we give a short morphological description of the structures detected in a sample of 28 early-type galaxies for which the main parameters are summarized in table I. This sample is only a part of a much larger sample of 114 objects which will be discussed elsewhere. In fig. 2-11 we show both the original image and the L-image for all galaxies in the sample; the morphologies are discussed together with all the information (mainly drawn from the literature) obtained via more traditional photometric and kinematical techniques. The images in fig. 2-11 are part of the *Atlas of Structures in Early-type Galaxies* which is also accessible via world wide web at the AIP (Astrophysikalisches Institut Potsdam [59]).

## 6. – Features in the sample galaxies

NGC 596: (fig. 2*a*)). – This galaxy is highly structured and is characterized by very pronounced twisting ($\sim 90°$) and by the presence of many ripples in the outer regions. From the detailed velocity field, Williams [60] concluded that it is a triaxial system which tends to become prolate in the outer regions. Several independent evidences suggest instead that a multicomponent structure provides a rather natural explanation for the observed morphology.

The isophotal geometry, studied in detail by several authors [26, 61-63] shows a variety of trends: isophotes are disky in the outer regions (outside of 20″) and turn mildly boxy in the intermediate ones, to turn again disky in the inner ones (inside 5″).

TABLE I. – *Main parameter for the sample galaxies.* 1) NGC *identification number*; 2) *morphological type taken from* RC3 [64]; 3) *distance in* Mpc *from Tully* [65] ($H_0$ *is* 75 km s$^{-1}$ Mpc$^{-1}$); 4) *absolute B magnitude*; 5) *dimension in* pc *of* 1″ *angular size.*

| Identification (1) | Type (2) | Distance (3) | $M_B$ (4) | pc (5) |
|---|---|---|---|---|
| NGC 596 | E pec | 23.8 | − 20.22 | 115 |
| NGC 636 | E3 | 24.2 | − 19.71 | 117 |
| NGC 1316 | PLXS0 | 16.9 | − 21.47 | 82 |
| NGC 1373 | E | 16.9 | − 17.02 | 82 |
| NGC 1374 | E | 16.9 | − 18.84 | 82 |
| NGC 1375 | S0 | 16.9 | − 17.94 | 82 |
| NGC 1389 | EX/S0 | 16.9 | − 18.75 | 82 |
| NGC 1549 | E0+ | 13.4 | − 19.77 | 65 |
| NGC 1553 | LAR0 | 13.4 | − 20.17 | 65 |
| NGC 4105 | E3 | 28.9 (a) | − 20.43 | 140 |
| NGC 4106 | S0 pec | 28.9 (a) | − 20.18 | 140 |
| NGC 4645 | E+ | 46.4 | − 21.03 | 225 |
| NGC 4696 | E1 pec | 46.4 | − 22.05 | 225 |
| NGC 4767 | E | 46.4 | − 21.13 | 225 |
| NGC 5574 | $S0_1$(8) | 28.7 | − 19.13 | 139 |
| NGC 5576 | E3 | 26.4 | − 20.40 | 128 |
| NGC 5638 | E1 | 28.4 | − 20.12 | 138 |
| NGC 6861 | LAS | 35.5 (a) | − 20.80 | 172 |
| NGC 6861D | LAS | 35.5 (a) | − 19.37 | 172 |
| NGC 6868 | E2 | 35.5 | − 21.06 | 172 |
| NGC 7144 | E0 | 24.8 | − 20.36 | 120 |
| NGC 7145 | E0 | 23.8 | − 19.81 | 115 |
| NGC 7155 | LBR0 | 23.5 | − 19.06 | 114 |
| NGC 7173 | E pec | 32.1 | − 19.47 | 156 |
| NGC 7176 | E pec | 32.1 | − 19.68 | 156 |
| NGC 7617 | LA0 | 48.9 (a) | − 18.7 | 237 |
| NGC 7619 | E3 | 45.9 | − 21.21 | 223 |
| NGC 7634 | LB | 38.2 | − 19.34 | 185 |

(*a*) The distance is computed from the average of the red-shift.

At the same radii abrupt variations in the PA of the isophotal major axis are also observed. This evidences together with the absence of obvious dust features which could mislead the interpretation [66, 67, 15] led Nieto *et al.* [26] to suggest that NGC 596 can harbour a weak bar similar to that observed in the prototype SB0 galaxy UGC 2656.

Michard and Marchal [63] suggested instead the existence of a peculiar disk. Surprisingly enough, no structure is listed for this galaxy in the survey by Ebneter *et al.* [68].

Schweizer and Seitzer [21] found a fine-structure parameter $\Sigma = 4.60$ and from the colors concluded that substantial rejuvenation of the galaxy must have occurred.

The L-Mor of NGC 596 (fig. 2*b*) and *c*)) turns out to be rather complex, the most striking feature being a rather disrupted asymmetric disk at PA = 50° *i.e.* coincident with the photometric major axis. This disk extends from about 20″ to about 42″ in the

Fig. 2. – *a*) NGC 596, original (ESO-NTT, *I*-band); *b*) NGC 596, Laplacian, outer regions; *c*) NGC 596, Laplacian, inner regions; *d*) NGC 636, original; *e*) NGC 636, Laplacian. All images —if not explicitly noted—were obtained at the NTT in the *I*-band. The bar at the bottom of each picture is 30″ long.

NE direction and from 20″ to 65″ in the SW one. Inside this region there is a tiny stellar disk (3″ in radius) at PA = 118°. The existence of this disk is confirmed by the high-resolution HST data presented in Lauer *et al.* [69]. Even though they failed to detect the disk, from their fig. 6 it is apparent that in the inner 3″, the isophotes turn disky and the PA of the major axis twists toward ∼ 120°. Two symmetric "blobs" laying at the same PA of the inner disk and at a distance of ∼ 14″ are also visible (fig. 2*c*)). They may, however, be an artifact introduced by the strong twisting. The overall

L-Mor is very similar to that of NGC 3384 [56]. As expected, no dust features are detected.

NGC 636: (fig. 2*d*)). – As far as isophotal properties are concerned, this galaxy is almost a twin to NGC 596. Franx *et al.* [70] and Nieto *et al.* [26] found strong twisting (45°), and an irregular behaviour of the Fourier coefficients between 15″ and 30″, which led them to conclude that this galaxy could host a faint bar-like structure oriented at PA = 75° plus a weak inner disk. The similarity to NGC 596 is further strengthened by the relatively high fine-structure index found by Schweizer and Seitzer [21], $\Sigma = 2.30$. The L-image (fig. 2*e*)) shows only a small, symmetric ring with a radius of 18.5″ at PA = 60°. This structure, however, is so faint that it is not a likely explanation for the photometric anomalies found by Nieto *et al.* [26].

NGC 1373: (fig. 3*a*)). – For this galaxy of the Fornax cluster Caon *et al.* [35] found a small variation in the Fourier coefficients at $\sim 15''$ which is explained as an artifact introduced by the poor removal of a rather bright edge-on spiral partially overlapping the galaxy on its *N* side. A more likely explanation however, is the very faint and inhomogeneous ring or edge-on ripple (PA = 72°) visible in the L-image (fig. 3*b*)). This feature appears to be slightly misaligned with respect to the major axis and is much more pronounced in the *B*-band rather than in the *I*-band frame.

NGC 1374: (fig. 3*c*)). – Member of the Fornax cluster, and forming a pair with NGC 1375, it has rather round isophotes with no systematic trend in the Fourier coefficients. Its kinematical properties [71] lead to conclude that it is more likely a close–to–face-on S0 galaxy, possibly hiding an inner weak counter-rotating disk component [72, 73]. The L-image (fig. 3*d*)) presents indeed a small and weak elongated feature ($r \sim 3''$ and PA = 50°) which could correspond to the above disk.

NGC 1375: (fig. 3*e*)). – In Fornax cluster and forming a pair with NGC 1374, it is an edge on S0 with a very boxy inner bulge. The photometric study by Caon *et al.* [35] shows mixed behaviour: in the intermediate regions, *i.e.* between $\sim 5''$ and $\sim 15''$ the isophotes are boxy, while outside of this range they are markedly disky. When inspected carefully the isophotes of this galaxy appear X-shaped, rather than boxy.

Phillips *et al.* [74] detected some nulcear, highly flattened $H_\alpha$ emission, as in the case of NGC 128, the classical peanut-shaped galaxy [75].

The complex L-Mor (fig. 3*f*)) of this object has already been discussed by Lorenz *et al.* [57] who used it to understand the anomalous values found for the amplitude of the surface brightness fluctuations. The L-Mor provides a clear explanation for the observed photometric characteristics: a well-pronounced outer disk with PA = 90° and extending from 2.5″ to about 40″, and inside this disk an inner dust ring with $r = 9.5''$. The dust lane occurs exactly at the same distance where the $a_4$ coefficient shows the largest degree of "boxiness".

The most remarkable feature is the strong "flare" observed in the outer disk, where the scale height changes from $\sim 2.5''$ to $\sim 7''$ reaching the maximum value at $\sim 12''$ from the nucleus. Presently, it is not yet clear if the "flare" is connect with the presence of the X structure or is an artifact of the filter.

There are also some indications for an inner disk: about 2″ long and with the same PA ($\sim 90°$) of the major axis. This inner disk is very likely produced by the excess emission coming from the disk of ionized gas. This disk within a disk structure appears

Fig. 3. – *a*) NGC 1373, original; *b*) NGC 1373, Laplacian; *c*) NGC 1374, original; *d*) NGC 1374, Laplacian; *e*) NGC 1375, original; *f*) NGC 1375, Laplacian. All images—if not explicitly noted —were obtained at the NTT in the *I*-band. The bar at the bottom of each picture is 30″ long.

to be very similar to that detected using HST data by van den Bosh *et al.* [76] in NGC 4570.

NGC 1316: (fig. 4*a*)). – This is the well-known Fornax A galaxy for which in the literature an impressive amount of data exists. We shall summarize here only those aspects which are relevant to the present topic. It possesses a highly structured radio loud nucleus and displays a whole variety of tails and filaments in the outer regions plus ripples and a chaotic distribution of gas and dust in the inner ones (*e.g.* [15]. These

Fig. 4. – *a*) NGC 1316, original; *b*) NGC 1316, Laplacian; *c*) NGC 1316, Gradient; *d*) NGC 1549, original; *e*) NGC 1549, Laplacian, outer regions; *f*) NGC 1549, Laplacian, inner regions. All images—if not explicitly noted—were obtained at the NTT in the *I*-band. The bar at the bottom of each picture is 30″ long.

characteristics together with its central velocity dispersion which is significantly lower than that of galaxies having similar luminosity are strongly suggestive of a very recent or still ongoing merger.

The L-Mor (fig. 4*b*)) of the inner regions is extremely complex and reveals the same intricate pattern of dust features observed with more traditional techniques. Some of these structures have roughly circular symmetry and seem related to the system of shells (at 44″, 91″ and 168″ from the center) which are clearly visible in the Gradient

Fig. 5. – *a*) NGC 1389, original; *b*) NGC 1389, Laplacian; *c*) NGC 1553, original; *d*) NGC 1553, Laplacian; *e*) NGC 4105 and NGC 4106, original; *f*) NGC 4105 and NGC 4106, Laplacian. All images—if not explicitly noted—were obtained at the NTT in the *I*-band. The bar at the bottom of each picture is 30″ long.

image shown at a smaller scale in fig. 4*c*). In the inner parts we see a weak bar/disk signature with a patchy appearance produced by the absorption features.

NGC 1389: (fig. 5*a*)). – The object has a complex L-Mor (fig. 5*b*)), the strongest feature being a well-defined inner disk with PA = 38° and 7″ radius. At the same PA but with a radius of 30″ there is the weak signature of a stellar ring. An intermediate ring, with a radius of 11″, is slightly misaligned (PA = 6°).

Fig. 6. – *a*) NGC 4645, original (ESO-NTT, *V*-band); *b*) NGC 4645, Laplacian; *c*) NGC 4696, original; *d*) NGC 4696, Laplacian; *e*) NGC 4767, original (ESO-NTT, *V*-band); *f*) NGC 4767, Laplacian. All images—if not explicitly noted—were obtained at the NTT in the *I*-band. The bar at the bottom of each picture is 30″ long.

NGC 1549 and NGC 1553: (fig. 4*d*) and 5*c*)). – It is a wide pair of moderately interacting galaxies. Malin and Carter [19] found around each of them faint structured envelopes containing ripples (one is 5′ E of NGC 1549 and another one is 5′ N of NGC 1553) and a faint jet (protruding westward of NGC 1553). Due to the scale, both these structures cannot be detected on our frames. Goudfrooij and de Jong [67] found a very small amount of dust which is very likely to be diffuse.

NGC 1549 has a rather strong twisting, from $\sim 100°$ in the very inner regions to about 145° at $\sim 40''$, while the isophotes are boxy in the intermediate regions to become disky outside of 40″ [26]. The L-image NGC 1549 (fig. 4*e*)) shows a variety of structures: first of all, two asymmetric blobs of enhanced emission (PA = 156°, $r = 50''$) which explain both the isophotal shape parameter and the twisting trends. At a closer inspection (fig. 4*f*)) more structures appear in the inner regions: three symmetric rings with average radius of 9″ and PAs of 86°, 106° and 128°, respectively.

In the L-image of NGC 1553 (fig. 5*d*)) we detect a large and very well-defined ring crossed by several dust absorption features. Two tiny spiral arms protrude from the ring in the NE and SW directions. The complex morphology of NGC 1553 is completed by the two rather broad and well-defined spiral arms which are clearly visible.

NGC 4105 and NGC 4106: (fig. 5*e*)). – These two galaxies form a rather isolated close pair of interacting S0 galaxies. In spite of its being a rather intense X-ray source there is only one photometric study available in the literature [77] which, however, is limited to one color only and does not provide any information on the geometry of the isophotes. The L-image (fig. 5*f*)) clearly shows two inner stellar disks hidden in the central regions. The one in NGC 4105 has $r = 6''$ and PA = 92°, while that in NGC 4106 has $r = 5.8''$ and PA = 151°. The most striking features are seen around NGC 4105: the first one is a long ($\sim 1'$) straight and narrow tail protruding westward from a knot of enhanced emission located at $r = 23''$ and PA = 166°, a second more diffuse patch is at PA = 78° and has a faint westward extension $\sim 25''$ long; the third and last patch is located at PA = 314°.

NGC 4645: (fig. 6*a*)). – The only available photometric study of this galaxy [78] does not provide isophotal shape analysis. The L-image (fig. 6*b*)) shows a clearly visible stellar disk with PA = 55° which extends out to $r = 8.5''$. In the outer parts this disk appears disrupted into a ring with radius of 17.5″. On the west side only some weak "blobs" are also visible.

NGC 4696: (fig. 6*c*)). – In the L-image (fig. 6*d*)) we see a core ($r = 3.8''$) surrounded by a complex of faint structures resembling a disrupted spiral arm.

NGC 4767: (fig. 6*e*)). – Originally classified as an E5 galaxy, it actually is an S0/a [79] *et al.* 1994). This revised classification is confirmed by our L-image (fig. 6*f*) which clearly shows a rather extended and structured disk which harbors four nested rings or shells with apparent of identical flattening ($\varepsilon = 0.5$). The innermost structure appears as an elongated disk with $r = 5.9''$ and PA = 130°. The three rings occur at $r =$ 9.5″, 22.4″ and 26.2″. A fourth, asymmetric ring is at $r = 50''$.

NGC 5574: (fig. 7*a*)). – Interacting with NGC 5576, Schweizer and Seitzer [21] failed to detect any anomalous structure ($\Sigma = 0$). According to Michard and Marchal [63], this galaxy is surrounded by an envelope with pronounced spiral structure. The L-image (fig. 7*b*)) is characterized by an inner disk ($r = 4.5''$) and an outer, more extended feature ($r = 26.8''$; PA = 64°) with the appearance of either a bar or an extended, not perfectly edge-on stellar disk slightly warped at the extremities. Such warp may explain the spiral structure suspected by Michard and Marchal.

NGC 5576: (fig. 7*c*)). – It is a boxy elliptical with a rather bright core (well above the $r^{1/4}$ law). Michard and Marchal [63] found a peculiar envelope with marked twisting and strong asymmetries. No dust absorption is detected even though Goudfrooij and de Jong [67] found (from IRAS data) an appreciable amount of dust. In the L-image (fig. 7*d*)) we see an inner stellar disk ($r = 3''$) and an outer ripple ($r = 7''$).

NGC 5638: (fig. 7*e*)). – Ebneter *et al.* [68] found evidences for very weak diffuse dust. In the L-image (fig. 7*f*)) we see no structures at all.

NGC 6861: (fig. 8*a*)). – No detailed photometric studies are available for this object. In the L-image (fig. 8*b*)) we see a rather well-defined broad-disk signature. The disk has $r = 20''$ and PA = 140° and may be slightly warped at the extremities, a tendency which seems confirmed by the PA of the outer ring ($r = 27''$, PA = 143°). The inner regions (fig. 8*c*)) clearly show a system of two symmetric and co-planar dust rings ($r = 3.4''$ and $r = 8.3''$ with PA = 140°).

NGC 6861D: (fig. 8*d*)). – No detailed photometric studies are available. The asymmetric central feature visible in the L-image (fig. 8*e*)) is either a misaligned stellar disk or a bar. The butterfly-like appearance is produced by the overposition of the bulge and a rather thick disk (comprised between $r = 6.5''$ and $r = 16.5''$) with PA = 162°. The disk ends into a symmetry structure which can be interpreted as either an inclined ring or a shell at $r = 25''$.

NGC 6868: (fig. 9*a*)). – Deep multiband (*B* and *R*) imaging of this object has revealed the existence of an arc-shaped nuclear dust patch [80]. In the L-image (fig. 9*b*)) we clearly see the central absorbing patch with an elongated appearance ($r = 4.8''$ and PA = 56°).

NGC 7144: (fig. 9*c*)). – Almost round galaxy with no definite isophotal shape [81]. A small amount of dust (possibly diffuse) is detected by Goudfrooij and de Jong [67]. We found no structures in the L-image (fig. 9*d*)).

NGC 7145: (fig. 9*e*)). – The isophotal Fourier coefficients do not show any systematic trend. Due to its roundness, the determination of photometric parameters such as twisting and ellipticity profiles is rather difficult for this galaxy. There is, however, a well-defined minimum in the twisting profile at about 20″ from the center [70]. Franx *et al.* [82] also found a strong kinematical misalignment in the outer regions. A very weak shell, NW of the galaxy, has been detected by Malin and Carter [19], but it is outside of our field of view. The L-image (fig. 9*f*)) does not show any structure. This galaxy is therefore very likely to be a truly triaxial system.

NGC 7155: (fig. 10*a*)). – The L-image (fig. 10*b*)) shows an extended disk (PA = 96°) with scale-height increasing outwards: from $h = 1.5''$ at $r = 8''$ to $h = 3.8''$ at $h = 24''$. The central core appears elongated in direction PA = 165°.

Fig. 7. – *a*) NGC 5574, original; *b*) NGC 5574, Laplacian; *c*) NGC 5576, original; *d*) NGC 5576, Laplacian; *e*) NGC 5638, original; *f*) NGC 5638, Laplacian. All images—if not explicitly noted —were obtained at the NTT in the *I*-band. The bar at the bottom of each picture is 30″ long.

NGC 7173: (fig. 10*c*)) and NGC 7176 (fig. 10*e*)). – Both galaxies belong to the compact group Hickson 90. Detailed kinematical and photometric studies [83, 84] show that NGC 7173 is undergoing a phase of strong interaction with the late-type galaxy NGC 7174. These three galaxy form a subgroup which is very likely to be interacting with the fourth member of the group, NGC 7172 [85].

Both galaxies present very small inner disks in the L-image. The disk in NGC 7173 (fig. 10*d*)) has $r = 5''$ and PA = 62°, *i.e.* it is at the same PA of the outer isophotes. In

Fig. 8. – *a*) NGC 6861, original; *b*) NGC 6861, Laplacian, outer regions; *c*) NGC 6861, Laplacian, inner regions, *d*) NGC 6861D, original; *e*) NGC 6861D, Laplacian. All images—if not explicitly noted—were obtained at the NTT in the *I*-band. The bar at the bottom of each picture is 30″ long.

NGC 7176 (fig. 10*f*)) we find what looks like a tiny stellar disk ($r = 2.5''$, PA = 55°) with an overimposed dust feature. The intricate pattern of features dominating the lower part of fig. 10*f*) is the late-type galaxy NGC 7174 which appears severely distorted by the ongoing interaction with NGC 7173.

NGC 7617: (fig. 11*a*)). – No detailed photometric study is available for this object. In the L-image (fig. 11*b*)) we recognize an inner stellar disk ($r = 2.5''$ and

Fig. 9. – *a*) NGC 6868, original; *b*) NGC 6868, Laplacian; *c*) NGC 7144, original; *d*) NGC 7144, Laplacian; *e*) NGC 7145, original; *f*) NGC 7145, Laplacian. All images—if not explicitly noted—were obtained at the NTT in the *I*-band. The bar at the bottom of each picture is 30″ long.

PA = 34°), plus a disrupted ring with $r = 12.6''$ and PA = 36°. At larger radii visible a pattern of "blob"-like features is clearly.

NGC 7619: (fig. 11*c*)). – E3 galaxy with rather normal appearance. Both Ebneter *et al.* [68] and Schweizer and Seitzer [21] failed to detect any anomalous feature ($\Sigma = 0$). This galaxy has, however, a radio loud nucleus [86]. Photometric and kinematical prop-

Fig. 10. – *a*) NGC 7155, original; *b*) NGC 7155, Laplacian; *c*) NGC 7173, original; *d*) NGC 7173, Laplacian; *e*) NGC 7176, original; *f*) NGC 7176, Laplacian. All images—if not explicitly noted —were obtained at the NTT in the *I*-band. The bar at the bottom of each picture is 30″ long.

erties have been studied in detail by Bender *et al.* [28] and Franx *et al.* [70] who find it to be moderately disky in the outer regions. In the L-image (fig. 11*d*)) we detect an inner stellar disk ($r = 4.9''$ and PA = 36°) not coplanar with the main galaxy plane. This disk might be related to the fueling of the nuclear radio source. We also detect an outer ring ($r = 11''$, PA = 36°).

NGC 7634: (fig. 11*e*)). – This galaxy has been studied by Ebneter *et al.* [68] who classified it as an SB0 galaxy. In the L-image (fig. 11*f*)) we detect an elongated inner core

Fig. 11. – *a*) NGC 7617, original; *b*) NGC 7617, Laplacian; *c*) NGC 7619, original; *d*) NGC 7619, Laplacian; *e*) NGC 7634, original; *f*) NGC 7634, Laplacian. All images—if not explicitly noted —were obtained at the NTT in the *I*-band. The bar at the bottom of each picture is 30″ long.

($r = 3''$, PA = 115°), plus an elongated disk ($r = 18''$ and PA = 95°) which appears slightly asymmetric with respect to the nucleus and flaring at the extremities. This phenomenon may be the result of strong isophotal twisting of the bulge.

## 7. – Discussion

The variety of structures observed in the L-images (summarized in table II) can be grouped into a few classes: dust absorption features, outer stellar disks, inner stellar

disks, bars, ripples, and asymmetric features. In some of the sampled galaxies, several structures (if not all) coexist. The small number of objects discussed here prevents any accurate statistical discussion. Some crude percentages may, however, be derived: only three galaxies (*i.e.* 11% of the sample) lack any obvious signature of structures. Asymmetric features which seem to be induced by the interaction with a nearby companion are present in NGC 4105 and NGC 4696. In what follows we shall briefly discuss the various groups.

**7**˙1. *Galaxies with dust features.* – In our sample, only a few (4 out of 28) early-type galaxies present absorption features produced by dust. These features show up in the

TABLE II. – *Summary of detected features*: 1) *galaxy identification*; 2)-4) *summary of the detected structures divided in inner, intermediate and outer*.

| Identification | Inner structures | Intermediate structures | Outer structures |
|---|---|---|---|
| NGC 596 | misaligned inner disk | "blobs" | outer rings or disrupted disk |
| NGC 636 | — | small symmetric ring | — |
| NGC 1316 | very intricate inner structure | — | outer system of shells |
| NGC 1373 | weak stellar ring | — | — |
| NGC 1374 | weak inner disk | — | very weak outer ring |
| NGC 1375 | — | copplanar weak dust lane | large stellar disk with strong flaring |
| NGC 1389 | inner stellar disk | misaligned intermediate ring | outer ring |
| NGC 1549 | 3 misaligned inner rings | — | outer asymmetric "blobs" |
| NGC 1553 | inner spiral arms | — | disk with outer ring and spiral arms |
| NGC 4105 | inner stellar disk | — | tidal features |
| NGC 4106 | inner stellar disk | — | — |
| NGC 4645 | inner stellar disk | intermediate disrupted ring | "blobs" |
| NGC 4696 | extended core | — | disrupted spiral arms |
| NGC 4767 | inner stellar disk | 4 ripples | — |
| NGC 5574 | inner stellar disk | — | bar or disk slightly warped |
| NGC 5576 | inner stellar disk | 1 ring | 1 ring |
| NGC 5638 | — | no structures | — |
| NGC 6861 | 2 inner dust lanes | outer ring | strong stellar disk possibly warped |
| NGC 6861D | strong disk | disk | ripple |
| NGC 6868 | nuclear dust | — | — |
| NGC 7144 | — | no structures | — |
| NGC 7145 | — | no structures | — |
| NGC 7155 | central core | — | flaring stellar disk |
| NGC 7173 | inner stellar disk | — | — |
| NGC 7176 | inner stellar disk | dust feature | — |
| NGC 7617 | inner stellar disk | disrupted ring | outer "blobs" |
| NGC 7619 | inner stellar disk | — | outer ring |
| NGC 7634 | inner elongated core | extended bar/disk feature | — |

L-images as regions where a strong negative signature (see our conventions above) is followed by a positive plateau. This detection rate hardly compares with those found by Lauer *et al.* [69]. Our small detection rate clearly results from the fact that most frames where obtained in the *I*-band, *i.e.* in a spectral region where only the densest dust regions leave measurable signatures on the light distribution. Much higher detection rates are obtained at shorter wavelengths and in color maps [58]. We find two types of dust morphologies: structured lanes or rings (NGC 1375, NGC 6861) and nuclear patches (NGC 6868 and, possibly, NGC 7176).

**7**˙2. *Outer stellar disks.* – Outer stellar disks are detected in almost all S0 galaxies in our sample: NGC 1375, NGC 1553, NGC 5574, NGC 6861, NGC 7155 and NGC 7634. No outer disks are detected in the interacting pair of lenticulars NGC 4105 and NGC 4106, and in NGC 7617. While in the case of NGC 4105 this might just be the result of unfavorable orientation of the disk with respect to the line of sight as it is suggested by the symmetric distribution of what seems to be tidal patches, NGC 4106 is more likely an elliptical which has been misclassified due to the presence of some internal structures which will be discussed in the next paragraphs.

NGC 7617 appears as a structured elliptical where simple morphological classification is misled by the presence of strong ripples in the light distribution. The most striking features are however the strong "flares", *i.e.* sudden increases of the disks scale-lengths observed in NGC 1375 and NGC 7155. This flarings are similar to that observed in the disk of NGC 3115 by Capaccioli *et al.* [87] and seem to be a rather common phenomenon [58], but the possibility that the flare comes from an artifact of the filter in particular condition of the bulge and disk flattening should be checked through simulations.

The dumb-bell shape of the disk in NGC 7634 is likely to be an artifact introduced in the L-image by the strong isophotal twisting.

**7**˙3. *Galaxies with inner stellar disks.* – As inner stellar disks we denote all those highly flattened structures which are harbored in the inner regions of many ellipticals and extend less than $0.5R_e$. These disks are revealed in a large fraction of the sampled galaxies, both lenticulars (NGC 1389, NGC 7617, NGC 5574 and possibly NGC 1375) and ellipticals (NGC 596, NGC 1549, NGC 4105, NGC 4106, NGC 4645, NGC 4767, NGC 5576, NGC 7173, NGC 7176, and NGC 7619), *i.e.* in 23% of the S0s and in 60% of the Es.

**7**˙4. *Galaxies with ripples or stellar rings.* – First of all, we have to stress two aspects: the signature left by ripples in the L-Mor is in some extreme cases hardly distinguishable from that left by any faint structure producing two symmetric local maxima in the light distribution, such as, for instance, a ring or a bar (*e.g.* NGC 3384; [56]). Clear-cut ripples are detected in NGC 1316, NGC 4767, NGC 6861D and NGC 7617. Symmetric features which we interpret as either ripples or close-to-edge-on rings are detected in NGC 596. Ripple-like structures are detected in NGC 596, NGC 636, NGC 1373, NGC 1549, NGC 1389, NGC 4645, NGC 5576, NGC 7619, *i.e.* in almost 50% of the sampled galaxies.

* * *

PB and GR wish to thank the Director of the Capodimonte Astronomical Observatory for financial support during their stay at the OAC. This work was partially sponsored by the Italian Space Agency (ASI).

## REFERENCES

[1] TOOMRE A., in *IAU Symposium, No. 58, Formation and Dynamics of Galaxies*, edited by J. R. SHAKESHAFT (Reidel Publ. Co., Dordrecht) 1974, p. 405.
[2] BERTOLA F. and CAPACCIOLI M., *Astrophys. J.*, **200** (1975) 439.
[3] BINNEY J., *Mon. Not. R. Astron. Soc.*, **183** (1978) 501.
[4] CAPACCIOLI M. and LONGO G., *Astron. Astrophys. Rev.*, **5** (1994) 293.
[5] VAN ALBADA T. S., KOTANYI C. G. and SCHWARZSCHILD M., *Mon. Not. R. Astron. Soc.*, **198** (1982) 303.
[6] MERRIT D. and DE ZEEUW T., *Astrophys. J. Lett.*, **267** (1983) L19.
[7] TENJES P., BUSARELLO G., LONGO G. and ZAGGIA S., *Astron. Astrophys.*, **275** (1993) 61.
[8] TOOMRE A., in *Evolution of Galaxies*, edited by B. M. TINSLEY and R. LARSON (Yale University Press) 1977.
[9] QUINN P. J., *Astrophys. J.*, **279** (1984) 596.
[10] DUPRAZ C. and COMBES F., *Astron. Astrophys.*, **166** (1986) 53.
[11] BARNES J. E. and HERNQUIST L., *Annu. Rev. Astron. Astrophys.*, **30** (1992) 705.
[12] SCHWEIZER F., *Astrophys. J.*, **252** (1982) 455.
[13] BARNES J. E., *Astrophys. J.*, **393** (1992) 484.
[14] SANDAGE A. R., *The Hubble Atlas of Galaxies* (Carnegie Inst., Washington) 1961.
[15] VAN DOKKUM P. G. and FRANX M., *Astron. J.*, **110** (1995) 2027.
[16] KORMENDY J. and DJORGOVSKI S., *Annu. Rev. Astron. Astrophys.*, **27** (1989) 235.
[17] MALIN D. F., *Nature*, **277** (1980) 279.
[18] MALIN D. F. and CARTER D., *Nature*, **285** (1980) 643.
[19] MALIN D. F. and CARTER D., *Astrophys. J.*, **274** (1983) 534.
[20] SCHWEIZER F. and SEITZER P., *Astrophys. J.*, **328** (1988) 88.
[21] SCHWEIZER F. and SEITZER P., *Astron. J.*, **104** (1992) 1039.
[22] DE VAUCOULEURS G. and CAPACCIOLI M., *Astrophys. J. Suppl.*, **40** (1979) 699.
[23] CAPACCIOLI M., in *IAU Symposium No. 127, Structure and Dynamics of Elliptical Galaxies*, edited by T. DE ZEEUW (Kluwer-Reidel, Dordrecht) 1987, p. 47.
[24] SIMIEN F. and DE VAUCOULEURS G., *Astrophys. J.*, **302** (1986) 564.
[25] RIX H.-W. and WHITE S. D. M., *Astrophys. J.*, **362** (1990) 52.
[26] NIETO J.-L., BENDER R., POULAIN P. and SURMA P., *Astron. Astrophys.*, **257** (1992) 97.
[27] BENDER R., DÖBEREINER S. and MÖLLENHOFF C., *Astron. Astrophys. Suppl.*, **74** (1988) 385.
[28] BENDER R., SURMA P., DÖBEREINER S., MÖLLENHOFF C. and MADEJSKI R., *Astron. Astrophys.*, **217** (1989) 35.
[29] MIYAMOTO M. and NAGAI R., *Publ. Astron. Soc. Jpn.*, **27** (1975) 533.
[30] JAFFE W., FORD H. C., O'CONNELL R. W., VAN DEN BOSCH F. C. and FERARESE L., *Astron. J.*, **108** (1994) 1567.
[31] CAPACCIOLI M., CAON N. and D'ONOFRIO M., *Mon. Not. R. Astron. Soc.*, **259** (1992) 323.
[32] HAMABE M. and KORMENDY J., in *IAU Symposium No. 127, Structure and Dynamics of Elliptical Galaxies*, edited by T. DE ZEEUW (Kluwer-Reidel, Dordrecht) 1987, p. 379.
[33] CAPACCIOLI M., CAON N. and D'ONOFRIO M., in *Structure, Dynamics and Chemical Evolution of Elliptical Galaxies*, edited by J. DANZIGER *et al.* (ESO, Munich) 1993, p. 43.
[34] CAPACCIOLI M., HELD E. V., LORENZ H., RICHTER G. and ZEINER R., *Astron. Nachr.*, **309** (1988) 69.

[35] CAON N., CAPACCIOLI M. and D'ONOFRIO M., *Astron. Astrophys. Suppl.*, **106** (1994) 199.
[36] KENT S. M., *Astrophys. J. Suppl.*, **59** (1985) 115.
[37] ZEPF S. E., WHITMORE B. C. and LEVISON H. F., *Astrophys. J.*, **383** (1991) 524.
[38] MICHARD R., *Astron. Astrophys. Suppl.*, **59** (1985) 205.
[39] BETTONI D. and FASANO G., *Astron. J.*, **105** (1993) 1291.
[40] SCHNEIDER D. P., GUNN J. E. and HOESSEL J. G., *Astrophys. J.*, **268** (1983) 476.
[41] HOESSEL J. G. and SCHNEIDER D. P., *Astron. J.*, **90** (1985) 1468.
[42] SCHOMBERT J. M., *Astrophys. J. Suppl.*, **64** (1987) 643.
[43] THOMSEN B. and FRANDSEN S., *Astron. J.*, **88** (1983) 789.
[44] JORGENSEN I., FRANX M. and KJAERGAARD P., *Astron. Astrophys. Suppl.*, **95** (1992) 489.
[45] MALKAN M. A., MARGON B. and CHANAN G. A., *Astrophys. J.*, **280** (1984) 66.
[46] BINGGELI B. and CAMERON L. M., *Astron. Astrophys. Suppl.*, **98** (1993) 297.
[47] DAVIES J. I., PHILLIPS S., CAWSON M. G. M., DISNEY M. J. and KIBBLEWHITE E. J., *Mon. Not. R. Astron. Soc.*, **232** (1988) 239.
[48] SERSIC J. L., *Atlas des Galaxias Australes* (Observatorio Astronómico, Cordoba) 1968.
[49] CAON N., CAPACCIOLI M. and D'ONOFRIO M., *Mon. Not. R. Astron. Soc.*, **265** (1993) 1013.
[50] DJORGOVSKI G. and DAVIS M., *Astrophys. J.*, **313** (1987) 59.
[51] AGUILAR L. and WHITE S. D. M., *Astrophys. J.*, **295** (1985) 374.
[52] BURT P. and ADELSON E., *IEEE Trans. Commun.*, **31** (1983) 532.
[53] RICHTER G. M., *Astron. Nachr.*, **299** (1978) 283.
[54] CAPACCIOLI M., PIOTTO G. P. and RAMPAZZO R., *Astron. J.*, **96** (1988) 482.
[55] LORENZ H., RICHTER G., CAPACCIOLI M. and LONGO G., *Astron. Astrophys.*, **277** (1993) 321.
[56] BUSARELLO G., CAPACCIOLI M., D'ONOFRIO M., LONGO G., RICHTER G. M. and ZAGGIA S., *Astron. Astropys.* (1996), in press.
[57] LORENZ H., BÖHM P., CAPACCIOLI M., RICHTER G. M. and LONGO G., *Astron. Astrophys.*, **277** (1993) L15.
[58] BÖHM P., CAPACCIOLI M., LONGO G., RICHTER G. M. and D'ONOFRIO M., *Astron. Astrophys.* (1997*a*) in preparation.
[59] BÖHM P., CAPACCIOLI M., LONGO G., RICHTER G. M. and D'ONOFRIO M., *Atlas of Structures in Early-Type Galaxies* (1997*b*). www URL: http://www.aip.de:8080/science/Atlas.htlm.
[60] WILLIAMS T. B., *Astrophys. J.*, **244** (1981) 438.
[61] CARTER D., *Astrophys. J.*, **312** (1987) 514.
[62] NIETO J.-L. and BENDER R., *Astron. Astrophys.*, **215** (1989) 266.
[63] MICHARD R. and MARCHAL J., *Astron. Astrophys. Suppl.*, **105** (1994) 481.
[64] DE VAUCOULEURS G., DE VAUCOULEURS A., CORWIN H. G., BUTA R. J., PATUREL G. and FOUQUÉ P., *Third Reference Catalogue of Bright Galaxies* (Springer, New York, N.Y.) 1991.
[65] TULLY B., *Atlas of Nearby Galaxies* (Cambridge University Press.), 1988.
[66] VERON-CETTY M. P. and VERON P., *Astron. Astrophys.*, **204** (1988) 28.
[67] GOUDFROOIJ P. and DE JONG T., *Astron. Astrophys.*, **298** (1995) 784.
[68] EBNETER K., DJORGOVSKI S. and DAVIS M., *Astron. J.*, **95** (1988) 422.
[69] LAUER T. R., AJHAR E. A., BYUN Y.-I., DRESSLER A., FABER S. M., GRILLMAIR C., KORMENDY J., RICHSTONE D. and TREMAINE S., *Astron. J.*, **110** (1995) 2622.
[70] FRANX M., ILLINGWOTH G. and HECKMAN T., *Astron. J.*, **98** (1989*a*) 538.
[71] D'ONOFRIO M., ZAGGIA S., CAON N. and CAPACCIOLI M., *Astron. Astrophys.*, **296** (1995) 319.
[72] VAN DER MAREL R. P. and FRANX M., *Astrophys. J.*, **407** (1993) 525.
[73] LONGO G., ZAGGIA S., BUSARELLO G. and RICHTER G. M., *Astron. Astrophys. Suppl.*, **105** (1994*a*) 433.
[74] PHILIPPS M. M., JENKINS C. R., DOPITA M. A., SADLER E. M. and BINETTE L., *Astron. J.*, **91** (1986) 1062.
[75] D'ONOFRIO M., CAPACCIOLI M. and MERLUZZI P., 1997, in preparation.

[76] VAN DEN BOSH F. C., FERRARESE L., JAFFE W., FORD H. C. and O'CONNELL R. W., *Astron. J.*, **108** (1994) 1579.
[77] DE CARVALHO R. R. and DA COSTA L. N., *Astrophys. J. Suppl.*, **68** (1988) 173.
[78] PENEREIRO J. C., DE CARVALHO R. R., DJORGOVSKI S. and THOMPSON D., *Astron. Astrophys. Suppl.*, **108** (1994) 461.
[79] NIETO J.-L., POULAIN P. and DAVOUST E., *Astron. Astrophys.*, **283** (1994) 1.
[80] HANSEN L., JORGENSEN H. E. and NOORGARD-NIELSEN H. U., *Astron. Astrophys.*, **243** (1991) 49.
[81] JORGENSEN I., FRANX M. and KJAERGAARD P., *Mon. Not. R. Astron. Soc.*, **273** (1995) 1097.
[82] FRANX M., ILLINGWOTH G. and HECKMAN T., *Astrophys. J.*, **344** (1989*b*) 613.
[83] LONGO G., BUSARELLO G., LORENZ H., RICHTER G. M. and ZAGGIA S., *Astron. Astrophys.*, **282** (1994*b*) 418.
[84] LONGO G., GRIMALDI A. and RICHTER G. M., *Astron. Astrophys.*, **289** (1995) L45.
[85] LONGO G., BUSARELLO G., RICHTER G., MALIN D. and SHAKER A., 1997, in preparation.
[86] BIRKINSHAW M. and DAVIES R. L., *Astrophys. J.*, **291** (1985) 32.
[87] CAPACCIOLI M., CAPPELLARO E., HELD E. V. and VIETRI M., *Astron. Astrophys.*, **274** (1993) 69.